A UAV-borne magnetic survey for archaeological prospection of a Celtic burial site

Volkmar Schmidt[1*], Michael Becken[1] and Jörg Schmalzl[1] test how close the quality of a UAV-borne magnetic survey is to an archaeo-magnetic survey on the ground.

Introduction

The use of unmanned aerial vehicles (UAV) for magnetic measurements has increased rapidly in the last years. Driven by the demand for small-sized magnetic surveys for mineral exploration, numerous systems that use a UAV as a flying sensor platform have been developed and tested (Cunningham et al., 2018; Malehmir et al., 2017; McBarnet, 2005; Parshin et al., 2018; Tezkan et al., 2011).

In archaeological prospection, magnetic surveying has become a routinely used method. Since the targets are very small and shallow, the magnetic field has to be mapped very regularly, with small spacing, and close to the ground. When an area is covered with dense vegetation or is not walkable for any other reasons, a terrestrial measurement is not possible. Therefore, magnetic anomaly maps of many archaeological sites are patchy. UAV-borne magnetic surveys could help to complete these maps and they would enable the prospection of many areas with restricted accessibility on the ground.

While fixed-wing UAVs have the advantage of a large cruising range, multi-rotor UAVs are especially suited for very-near-surface exploration, since they can fly at very low speed and altitude. Low speed allows for a very dense spatial sampling in the sub-meter range and flying at low altitude allows for the detection of shallow magnetized bodies whose magnetic anomalies decay very quickly with increasing altitude.

There are now several lightweight magnetic measurement systems available on the market that can be lifted by a medium-sized UAV and make airborne measurements possible to accomplish for a wide range of users. The systems use either fluxgate magnetometers or optically pumped magnetometers. Both offer high sensitivity in the pico-Tesla range and fast sampling rates. However, these features alone do not guarantee a high-quality result in practice.

Figure 1 Magnetic measurement system ready for take-off.

There are a number of effects, which need to be considered in order to get an accurate magnetic anomaly map. The UAV generates electromagnetic noise, the sensor changes orientation quickly and the geodetic position of the sensors needs to be accurately determined in all three dimensions. When mapping a small-sized area, the ability of the UAV and the pilot to fly on equally spaced flight lines plays a major role for a regular sampling of the area. The demands are especially high, when the magnetic anomalies of interest have a small amplitude and wavelength. This is the case in archaeo-magnetic prospection, where the amplitude of the anomalies are often only a few nano-Tesla and the line spacing as low as 0.25 m. In this study, we tested how close the quality of a UAV-borne magnetic survey is to an archaeo-magnetic survey on the ground. A UAV-borne measurement was undertaken on an archaeological site that had been surveyed on the ground several years before.

Design of measurement system

Multi-rotor UAVs are especially suitable for small-scale surveys, since their flight path and speed can be accurately defined and steering is relatively simple. For the survey, we used an 8-rotor copter (DJI S1000+) with a payload of 5 kg (Figure 1). The original flight controller was replaced by a model, which allowed better integration of third-party sensors (Pixhawk 2.1). A differential GPS antenna (RTK-GPS Here+) was integrated. The GPS module on the UAV receives correction data during the flight from a GPS base station on the ground. This allows the copter to follow a pre-defined route with centimetre-accuracy. A laser range finder (Garmin LIDAR-Lite) measures the distance from the UAV to the ground and this data is used to fly with constant altitude above ground. Data from all sensors is logged in the flight controller and the log can be downloaded after the flight.

The total magnetic field is measured by a cesium-vapour magnetometer (MagArrow by Geometrics Inc.) with a sampling frequency of 1000 Hz and a sensitivity of 5 pT/√Hz. The magnetometer as well as a GPS antenna, a compass, and an inertial

[1] Institute for Geophysics, University of Münster
[*] Corresponding author, E-mail: volkmar.schmidt@uni-muenster.de
DOI: 10.3997/1365-2397.fb2020061

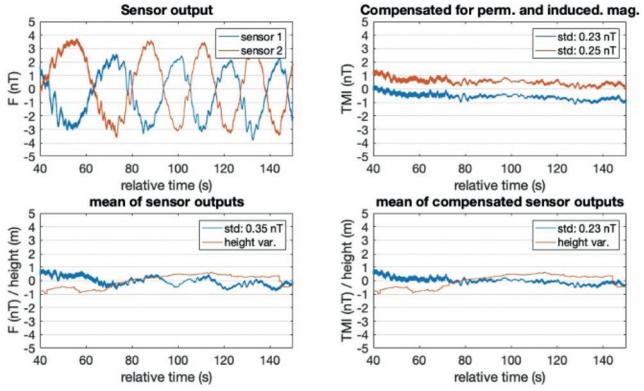

Figure 2 Variation of measured fields during a circular flight. Left side: Variation of data (heading error) for the individual sensors and the mean. Right: Compensated data for individual sensors and the mean of both sensors. The slight decrease of the values may be due to diurnal variation.

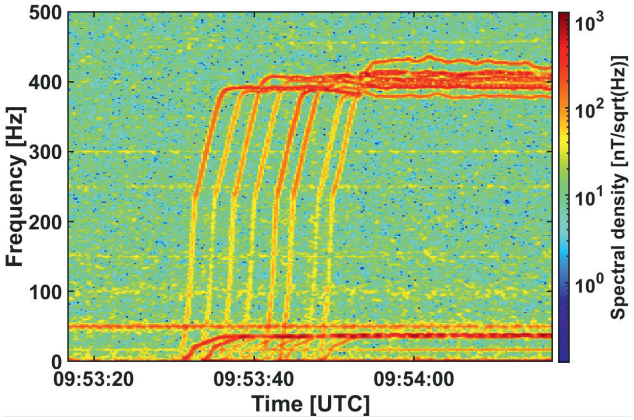

Figure 3 Frequency spectrum of the multi-copter at a distance of 1.2 m below the motors measured with an induction coil triple (SHFT02) and recorded with a sampling rate of 4096 Hz (ADU07e). The eight motors start successively after 09:53:30 UTC.

measurement unit (IMU) are enclosed in a carbon fibre bird. This device is attached to the UAV via 3m-long ropes. There is no data link between the UAV and the magnetic measuring system. Data from both devices have to be matched according to their GPS timestamps. These timestamps can have an offset, which must be accounted for during data processing.

The cesium magnetometer has some features that are advantageous for UAV-borne measurements. The measurement accuracy is only weakly affected by movement of the sensor and there is very little temperature drift. In archaeological prospection, fluxgate-gradiometers are often used to map the vertical gradient of the field, which is steepest close to the ground. But when the area is covered with vegetation and the sensor has to be flown at an altitude of some metres, measuring the total field will be beneficial, since the total field anomaly decays slower with increasing distance than the anomaly of the field gradient.

The employed magnetometer contains two miniaturized sensors with a heading error of ±5 nT according to the technical specifications. During a circular flight at high altitude with sensors oriented in opposite directions, the intrinsic heading error of each sensor was ±4 nT (Figure 2). Since the error had an opposite sign for the two sensors, the heading error could be reduced to ±1 nT by taking the mean of the two sensor readings. The heading error can be corrected more effectively when a mathematical compensation based on the attitude of the magnetometer is applied. This method by Leliak (1961) compensates for the effects of induced and permanent magnetization and it reduces the heading errors to a value of about 200 pT (Figure 2).

The influence of the aircraft on the magnetic measurements was tested extensively. For fixed-wing aircrafts, Leliak (1961) describes three different sources of magnetic inference and their relationship to the manoeuvres of an aircraft: permanent and induced magnetization of ferromagnetic parts, and magnetic fields produced by eddy currents in electrically conducting parts of the aircraft.

Fortunately, two of the sources can be neglected for our small-sized multi-copter. Induced magnetization is weak, since the UAV contains few ferromagnetic parts and existing ferromagnetic parts were replaced if possible. Fields due to eddy currents are also negligible, because unlike most airplanes the UAV has no electrically conducting frame and the cruising speed is very low. However, there are permanent magnets in the motors and additional interferences can occur due to strong and varying electrical currents from the batteries to the motors.

The brushless DC motors contain a number of strong permanent magnets. Since neighbouring magnets have opposite polarity, their magnetic stray fields cancel out partly. These magnets start to rotate when the engine is started and generate an alternating magnetic field. The frequency of this field depends on the design of the motor and the number of revolutions per minute. Our UAV shows noise at two frequencies in idle state (Figure 3). The peak at 36 Hz corresponds to the rotation frequency of the rotors and the peak around 400 Hz corresponds to the rotation frequency multiplied by the number of rotating magnet pairs. When hovering, frequency peaks at 76 Hz and 840 Hz are observed and these frequencies will be higher during the flight. Including magnetic fields from electrical currents, the influence of the UAV is a few nanotesla in a distance of 1 m, and it decays quickly with increasing distance. We found that it becomes insignificant when the distance is larger than 2.5 m.

Figure 4 shows the magnetic field data and flight parameters during a take-off. High-frequency noise is visible when the rotors are started and its amplitude varies during acceleration. When the UAV takes off, its distance from the magnetometer increases up to 3 m until the ropes are tight. Then the magnetometer is lifted into the air and has a constant distance from the UAV during the flight. The signal in Figure 4 also displays a permanent noise

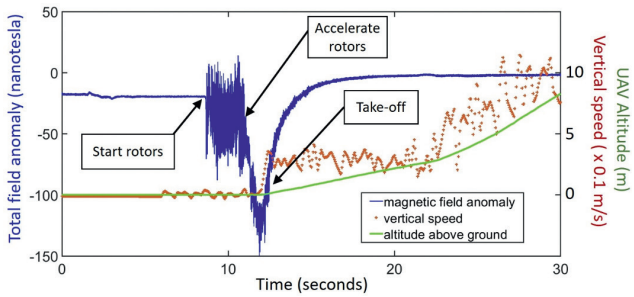

Figure 4 Magnetic field data during take-off. Altitude and vertical speed are from the flight controller log.

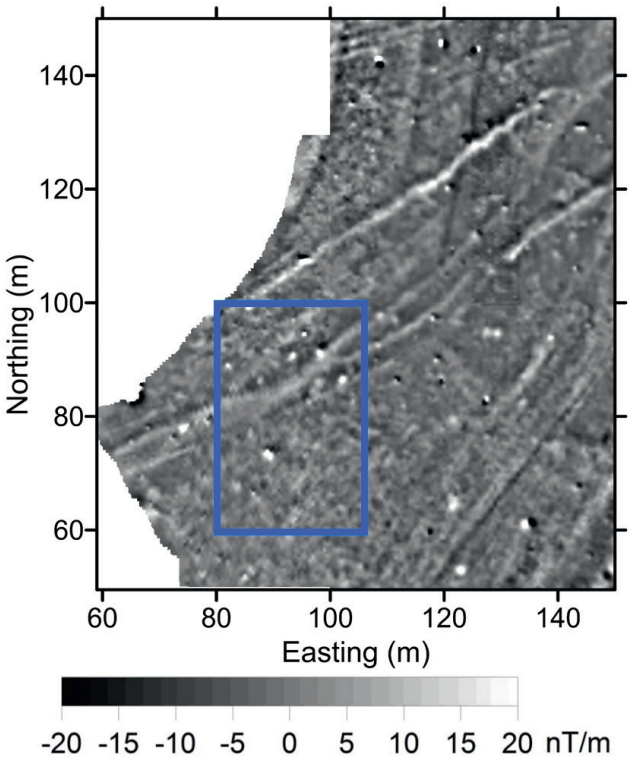

Figure 5 Magnetic anomaly map of the vertical (pseudo-) gradient of the total field, i.e. the difference of the total field values of the upper and lower sensors. The area outlined in blue is shown enlarged in Figure 6.

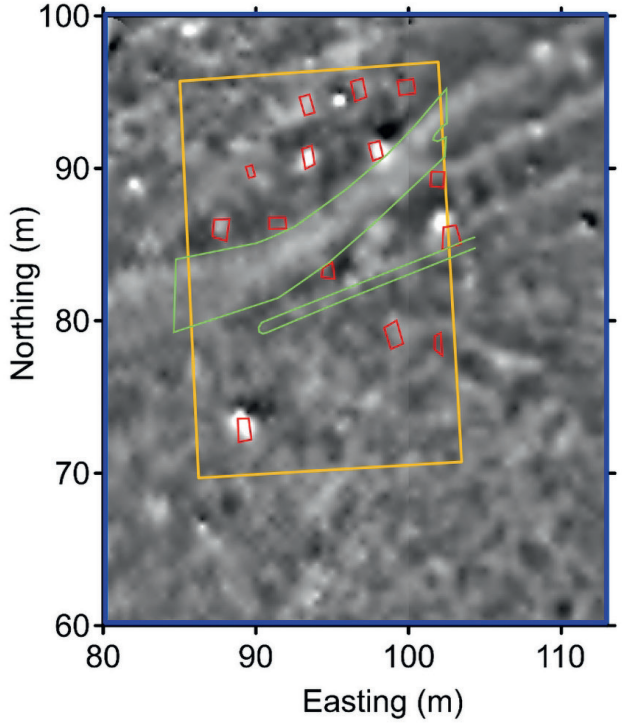

Figure 6 Subset of the anomaly map shown in Figure 5. The excavation area is outlined in yellow. Grave pits are shown in red.

from the power grid with frequency of 50 Hz and an amplitude of about 2 nT. This signal and other high-frequency noise can be suppressed by a 20 Hz low-pass filter. At 20 Hz, the sensor has a theoretical resolution of 25 pT. However, whether or not this value is reached during measurement can hardly be validated,

Figure 7 Flight plan of flight 33 with 1 m line spacing.

because the short-term variations of the Earth's magnetic field and the ambient noise field can be much larger.

The weak interference of the motors and the electric currents can also be compensated by the method of Leliak (1961). However, this requires that rotor speed, the relative position of the magnetometer to the UAV and electrical currents are constant. If this is not the case, much more complex correction routines would be required.

In practice, a careful flight planning helps to minimize these problems. The UAV should fly with constant speed and climb on straight lines to avoid noise amplitude variations. In the end, positioning errors may be more important for the quality of the result. Because when the magnetic field is sampled very close to the ground, the values can vary about several nanotesla per decimeter in all three spatial dimensions. The quality of positioning data is therefore decisive when flight altitudes are low and line spacing is only 1 m or less.

The archaeological site and ground survey

The survey site is a small forest glade with an area of about two hectares in the vicinity of a Celtic ringfort. Numerous burial sites from the La Tène period (about 450–0 BCE) have been found here based on a magnetic anomaly map (Gleser and Fritsch, 2016). The map was obtained by a ground magnetic survey in 2012 and 2013 using two cesium magnetometers in vertical gradiometer

mode and a sample spacing of 0.5 m. Except for some pieces of scrap, the maximum amplitude of the total field anomalies recorded by the lower sensor (about 30 cm above ground) was below 40 nT. The map of the vertical gradient (Figure 5) shows a variety of different anomalies, most of them with an amplitude below 20 nT/m. The source of some anomalies was verified by later excavations. The point-shaped anomalies with a diameter <3 m are caused by the burial sites or modern scrap (Figure 6). The distinction between the two is not simple, because some graves also contain antique iron objects. Subsequent excavations confirmed the existence of burial sites at most of the magnetic anomalies. The graves are found directly below the soil layer with a thickness of few centimetres. The anomaly of graves without iron objects is caused by filling the grave-pit with soil, which has a higher magnetic susceptibility than the bedrock. The linear, SW-NE-striking anomalies in the middle of the map are caused by a thicker layer of soil. Probably, they delineate ancient roads and are also of archaeological interest.

Figure 8 UAV-borne measurement with sensor very close to the ground.

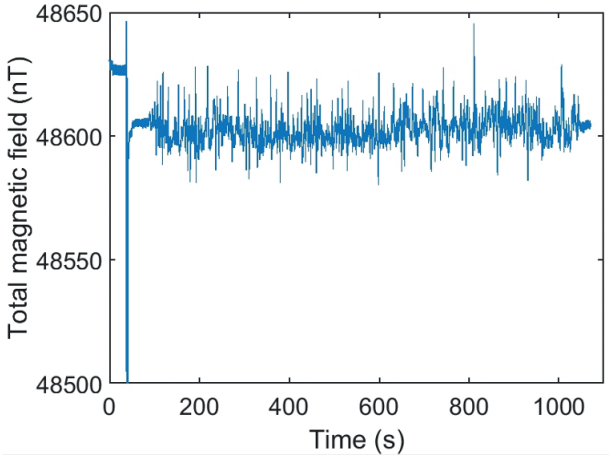

Figure 9 Raw data of flight 33. Recording was started in the 100s before take-off and stopped before landing.

UAV-borne survey

Because of the variety and characteristic pattern of magnetic anomalies, we chose the area as a test site for UAV-borne magnetic measurements. The survey would also show if the burial field extends farther towards the North. The area is surrounded by about 20 m-tall trees leading to limited number of GPS satellites in view. It shows differences in elevation of about 20 m. The flight path consisted of parallel profiles with 1m spacing (Figure 7).

In one flight, an area of 25 m x 50 m could be covered at a cruising speed of 2 m/s. After a flight time of about 20 minutes

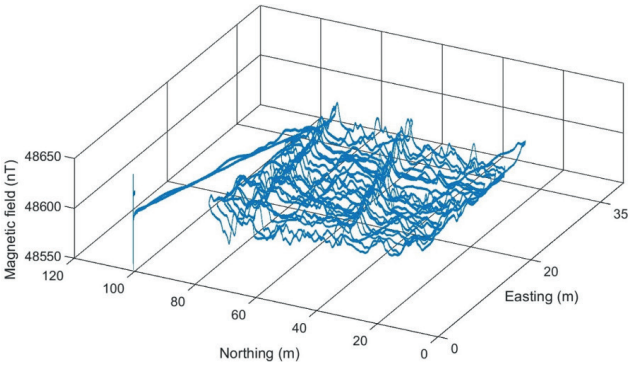

Figure 10 Spatial distribution of magnetic field data of flight 33.

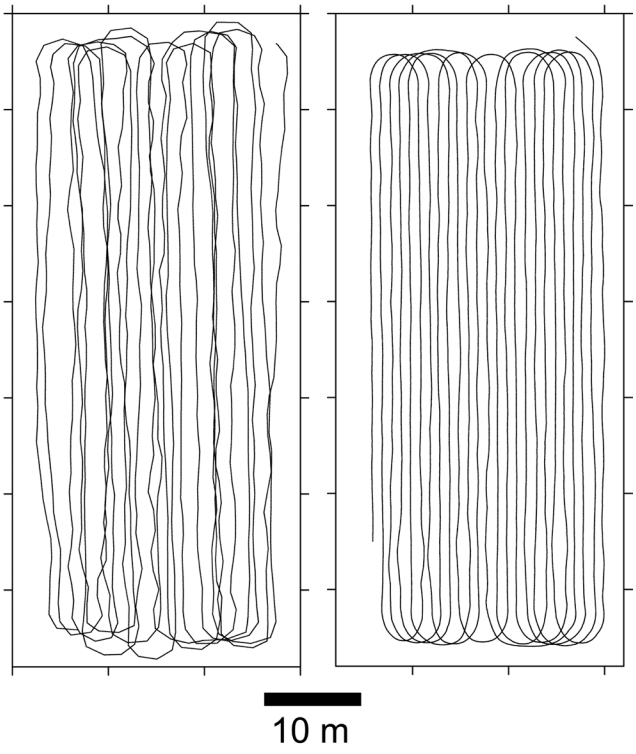

Figure 11 Plan view of flight path using GPS coordinates from the bird (left) and RTK-GPS coordinates from UAV (right) for flight 33.

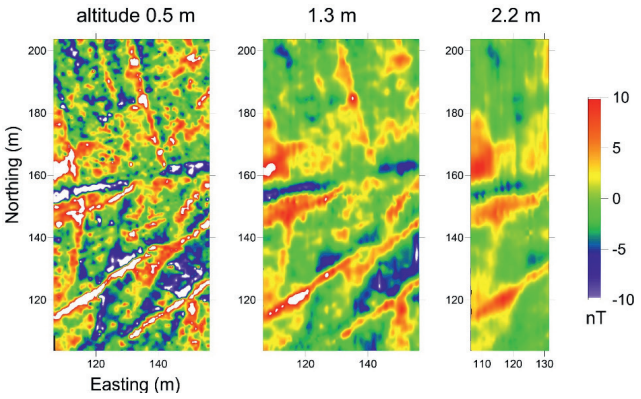

Figure 12 Total field anomaly maps after processing of flights at different altitudes.

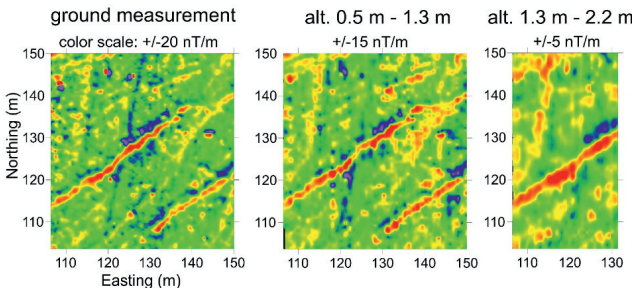

Figure 13 Comparison of vertical gradient map from ground measurement (left), difference of UAV-borne results measured at 0.5 m and 1.3 m altitude (middle) and difference of results from 1.3 m and 2.2 m altitude (right). Colour scale was chosen individually for better visual comparison of results. A scrap in the northern part has been removed after the ground measurements. The corresponding anomalies are therefore not visible in the UAV measurements.

the batteries needed to be recharged. The UAV kept a constant distance from the ground using its laser rangefinder. Since the magnetometer was situated directly beneath the UAV, the laser could not point vertically down, but was inclined 60° only. This resulted in slightly different flight altitudes above ground, when flying uphill or downhill. The flight lines were preferentially oriented normal to the slope to minimize this effect. The area was mapped at different altitudes with the magnetometer about 0.5 m, 1.3 m, and 2.2 m above the ground (Figure 8). This enabled us to derive vertical gradient maps, which usually show archaeological features most clearly. Temporal variations of the Earth's magnetic field were recorded by a proton precession magnetometer with an interval of 10 s.

Data processing and results

The data from flight 33 is shown in Figure 9 to Figure 11. The total field variations in the surveyed area are in a range of about 50 nT (Figure 9). A spatial plot of the magnetic raw data already shows clear linear anomalies (Figure 10). The coordinates that are recorded in the bird show less regular flight lines than the coordinates recorded by the RTK-GPS system on the UAV (Figure 11). This is mainly due to the higher accuracy of the RTK-GPS compared to the accuracy of the GPS in the bird, which is about 1 m. Although the real horizontal positions of the UAV and the bird may be offset by up to 1 m due to swinging of the bird, the coordinates of the UAV represent the flight path of the bird more accurately. The magnetometer sensors in the bird lag behind the position of the GPS antenna at the UAV by about 80 cm at a speed of 2 m/s. This was corrected in the data processing. The data was low-pass filtered and diurnal correction was applied. The magnetometer data was assigned to the GPS positions of the UAV and then gridded.

Figure 12 shows the total magnetic field anomaly maps at three different altitudes. The maximum amplitudes are 42 nT at 0.5 m altitude, 16 nT at 1.3 m and 10 nT at 2.2 m. With increasing altitude, the anomalies become weaker and smoother, but the main linear anomalies are well visible in all three maps.

The weak pattern of N-S-stripes in the data at 1.3 m and 2.2 m altitude probably result from slightly different flight altitudes in opposite directions and the gridding of data that have a much smaller inline spacing than line spacing.

Vertical pseudo-gradient maps were calculated by subtraction of the grids at different altitudes (Figure 13). The gradient map from flights at 0.5 m and 1.3 m altitude shows a remarkable similarity with the maps from the ground measurements. Virtually all anomalies from the ground measurements can be also discerned in the UAV-borne measurement, although the line spacing is coarser. Only the mapping of linear anomalies that have a similiar orientation like the flight lines is of lower quality. Another flight with perpendicular flight line orientation could improve the results, but also doubles measurement time.

The gradient map from flights at 1.3 m and 2.2 m altitude still shows the main anomalies (Figure 13). Elongated anomalies are clearly visible because they decay slower than small and isolated anomalies. A quantitative comparison of ground map and UAV-borne map was done after matching the scales and removing an offset betweeen the maps. The difference between the maps is then below 5 nT/m for 91% of the values and below 2 nT/m for 51% of the values. Large differences above 10 nT/m occur at places where the largest anomalies are situated and where pieces of scrap were removed in the time between the measurements.

Conclusions and outlook

The results have shown that UAV-borne magnetic measurements for near-surface exploration can compete with ground measurements, when the magnetometer can be flown very close to the ground. Because the UAV contains only few ferromagnetic parts, the magnetic interference is low. The main source of noise are the magnets in the rotors. They generate a high-frequency signal, which can vary with speed and distance to the magnetometer. High-frequency noise from the UAV and power grid was effectively filtered. The UAV offers the possibility of measuring the magnetic field at arbitrary altitudes above the ground, which enables the determination of the vertical gradient of the field. Even in altitudes of a few metres, many anomalies are discernable, especially when they show a larger extension. This makes a magnetic survey promising, also in areas where the bird has to keep a distance from the ground due to vegetation or other obstacles.

Exact position information of the magnetometer is very important in small-scale surveys. The integration of RTK-GPS in the bird would be desirable. Arrays of sensors would make the measurement more efficient, measurements with a smaller line spacing could be done efficiently and data consistency would be improved.

Although programming and flying a UAV has become feasible for many users nowadays, careful flight planning and an experienced pilot are needed to get high-quality magnetic data. In principle, arbitrary flight paths in three dimensions can be programmed and flown. Inversion of this kind of data will be challenging, but it can lead to new insights by imaging shallow subsurface structures in areas which have been not accessible by ground magnetic prospection until now.

Acknowledgements

We would like to thank Stefan Klingen and Stefan Ueding for their valuable contributions to the technical development. Raphaela Klafka and Philipp Kotowski are thanked for their contributions to the noise measurements and Thomas Fritsch for providing archaeological information on the site.

References

Cunningham, M., Samson, C., Wood, A. and Cook, I. [2018]. Aeromagnetic surveying with a rotary-wing unmanned aircraft system: A case study from a zinc deposit in Nash Creek, New Brunswick, Canada. *Pure and Applied Geophysics*, **175**, 3145-3158.

Gleser, R. and Fritsch, T. [2016]. Wein – Getreide – Rituale. Ausgrabungen in der spätkeltisch-frührömischen Nekropole Bierfeld „Vor dem Erker", Saarland. In: Koch, M. (Ed.) *Proceedings of Archäologentage Otzenhausen* **2**, 85-108.

Leliak, P. [1961]. Identification and evaluation of magnetic-field sources of magnetic airborne detector equipped aircraft. *IRE Transactions on Aerospace and Navigational Electronics* ANE-**8(3)**, 95-105.

Malehmir, A., Dynesius, L., Paulusson, K., Paulusson, A., Johansson, H., Bastani, M., Wedmark, M. and Marsden, P. [2017]. The potential of rotary-wing UAV-based magnetic surveys for mineral exploration: A case study from central Sweden. *The Leading Edge,* **36**(7)**,** 552-557.

McBarnet, A. [2005]. A little goes a long way with Fugro's latest unmanned aeromagnetic survey flying machine. *First Break,* **23**(2), 9-11.

Parshin, A.V., Morozov, V.A., Blinov, A.V., Kosterev, A.N. and Budyak, A.E. [2018]. Low-altitude geophysical magnetic prospecting based on multirotor UAV as a promising replacement for traditional ground survey. *Geo-Spatial Information Science,* **21**(1), 67-74.

Tezkan, B., Stoll, J.B., Bergers, R. and Großbach, H. [2011]. Unmanned aircraft system proves itself as a geophysical measuring platform for aeromagnetic surveys. *First Break,* **29**(4), 103-105.